AIChE

Equilibrium and Absorption Kinetics of Carbon Dioxide by Solid Supported Amine Sorbent

Esmail R. Monazam
REM Engineering Services, PLLC, 3537 Collins Ferry Rd., Morgantown, WV 26505

Lawrence J. Shadle and Ranjani Siriwardane
National Energy Technology Laboratory, U. S. Department of Energy, 3610 Collins Ferry Rd.,
Morgantown, WV 26507

DOI 10.1002/aic.12516

The equilibrium and conversion-time data on the absorption of carbon dioxide (CO_2) with amine-based solid sorbent were analyzed over the range of 303–373 K. Data on CO_2 loading on amine based solid sorbent at these temperatures and CO_2 partial pressure between 10 and 760 mm Hg obtained from volumetric adsorption apparatus were fitted to a simple equilibrium model to generate the different parameters (including equilibrium constant) in the model. Using these constants, a correlation was obtained to define equilibrium constant and maximum CO_2 loading as a function of temperature. In this study, a shrinking core model (SCM) was applied to elucidate the relative importance of pore diffusion and surface chemical reaction in controlling the rate of reaction. Application of SCM to the data suggested a surface reaction-controlled mechanism for the temperature of up to 40°C and pore-diffusion mechanism at higher temperature. Published 2011 American Institute of Chemical Engineers *AIChE J,* 57: 3153–3159, 2011
Keywords: adsorption gas, diffusion, gas purification, reaction kinetics, design

Introduction

Coal-fired power plants generate electricity by combusting coal to produce high pressure steam, which drives a series of turbines or generators. The coal combustion produces flue gas that contain carbon dioxide (CO_2) which is released to the atmosphere, a major greenhouse gas contributing to global climate change. The emission of CO_2 into atmosphere due to its large quantity has become one of the most serious environmental problems. To prevent the global warming by the greenhouse effect, the development of CO_2 capturing system and separating from the flue gases with a minimal energy penalty has attracted much attention nowadays.[1] The most widely established method to capture CO_2 is by chemical absorption using an aqueous solution of amine-based absorbents.[2] However, in the currently used systems, more than half of the capture cost is caused by absorbent regeneration. Therefore, to make these systems more cost effective, research scientists at NETL have developed a novel amine-based solid sorbents to remove CO_2 from flue gases.[3] However, no kinetic data are available for this promising sorbents. The knowledge of the kinetics data is of great importance in the design of CO_2 removal system, because it is related with solid inventory necessary in the absorber and regenerator reactors to transfer the CO_2 demanded in the regeneration reactor. The objective of this article is thus to determine the kinetic parameters of the CO_2 removal by amine-based solid sorbent. Therefore, this article discusses the equilibrium and kinetic model of CO_2 capture by amine-based solid sorbents. According to our best knowledge, this is the first equilibrium and kinetic investigation for amine-based solid sorbents.

Previous kinetic expressions on amine sorption are developed for aqueous solution or are volumetric in nature. As

---

Correspondence concerning this article should be addressed to L. J. Shadle at lshadl@netl.doe.gov.

such these expressions do not consider the effect that particle size of a solid supported sorbent has on the transport of CO_2 through the absorbed layer on the surface of particle. Yang and Hoffman[4] proposed that a commercial process would use particles as large as 500 μm diameter. It is well known that such particles will exhibit significant delays due to heat and mass-transport processes. There are a number of kinetic mechanisms which take these transport processes into account. These are considered and parameters are estimated to enable researchers to evaluate the feasibility of using such large size sorbents in these processes.

In all cases of gas absorption, there are two factors of fundamental importance which must be clearly kept in mind: (1) the equilibrium absorption or the maximum possible degree of absorption under given conditions of pressure, temperature, and concentration and (2) the rate of absorption. Both factors exert an important influence on the capacity of a solid supported sorbent and on the amount of sorbent needed in relation to the quantity of gas to be treated. The equilibrium concentration of the reacting gas establishes the driving force for the reaction rate. The sorbent itself has a capacity for the amount of gas that can be reacted that will be dependent on the temperature and reactant concentration. The extent that the sorbent attains that limit will be determined by reacting gas concentration and the equilibrium vapor pressure of the reacting gas over that sorbent. All of these parameters must be defined to describe the behavior of this amine supported sorbent for absorbing CO_2 and being regenerated to be recycled and used over and over again in a continuous commercial process.

Experiment

The equilibrium absorption was obtained using volumetric adsorption apparatus. Approximately 10 mL of the sorbent material was placed in the sample chamber and were evacuated to $\sim 5 \times 10^{-5}$ Torr at 25°C before each run. The amount of CO_2 adsorbed was calculated using pressure measurements before and after the exposure of the sample chamber to CO_2. Pressure measurements up to 103 Torr were obtained, using an MKS type 660 pressure gauge, and pressures >103 Torr were measured using a Setra Datum model 2000 pressure gauge. By measuring the pressure in this manner, it was possible to obtain more-accurate pressure measurements in the low-pressure region. For more details on the experimental procedure, see Siriwardane et al.[5]

To examine the fundamental kinetics of the fractional CO_2 conversions and rate of CO_2-uptake information using amine-based solid sorbent were carried out using Cahn 500 Thermomax 500 unit thermo-gravimetric analyzer (TGA). The solid sorbent was a mixture of amine and bentonite with specific gravities of 1.05 and 2.5, respectively, prepared using proprietary methods. The sorbent sample ($\sim$50 mg) was placed on the sample pan situated on the sample arm of the balance. This sample size minimized the depth of the sample layer in the pan to avoid any effects of intraparticle diffusion on the rate of weight gain in the sorbent. The mean sorbent particle diameter tested was 70 μm, the specific gravity was $\sim$1.7 using a volumetric mixing law and assuming no change in particle volume, and the surface area was determined assuming spherical particles.

Inert gas (N_2) was fed into weighing unit of the TGA to prevent the reactant gas from diffusing into the balance chamber. The temperature was ramped from 20°C to 100°C at 2.00°C/min. These sample were held at 100°C for 2 h before it was cooled back to the desired reaction temperature (30–100°C). The soak time during the pretreatment was increased from 30 to 120 min to obtain more reproducible weight change presumably a result of loss of residual water used during the impregnation of amine onto the bentonite support. The weight loss during the pretreatment soak at 100°C represented about 7.5% of the sample weight.

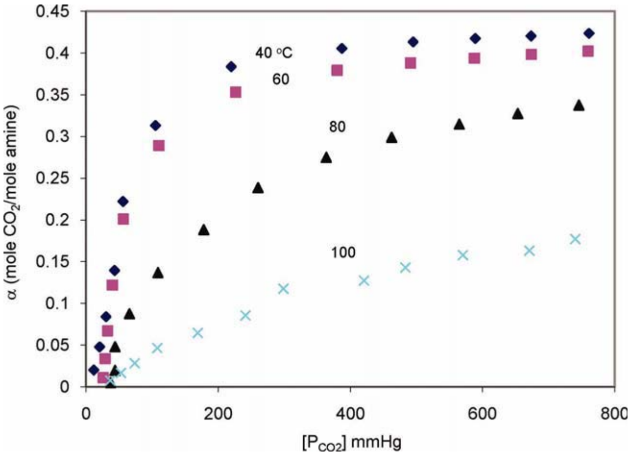

Figure 1. Experimental variation of CO_2 loading with equilibrium partial pressure.

[Color figure can be viewed in the online issue, which is available at wileyonlinelibrary.com.]

Results and Discussion

To compare the feasibility of the amine-based solid sorbent with other methods to remove CO_2 from flue gases, it is desirable to have available the fundamental data on equilibrium absorption and on absorption rates. The experimental CO_2 loading data, α, at different temperature and CO_2 partial pressure is shown by Figure 1. This data were correlated using following equilibrium model for each temperature:

$$\frac{d\alpha}{dC_{CO_2}} = -K_{eq}(\alpha_{CO_2} - \alpha_{max}) \tag{1}$$

Solving for the CO_2 loading (α) in Eq. 1 resulted in:

$$\alpha = \alpha_{max}\left(1 - e^{-K_{eq}C_{CO_2}}\right) \tag{2}$$

The values of K_{eq} and α_{max} were obtained by curve fitting the equilibrium data of Figure 1 with expression in Eq. 2 using TABLECURVE software available from SPSS. A typical fit of Eq. 2 to the CO_2 loading, α, measurements is illustrated by Figure 2. Agreement was very good over the entire CO_2 loading-CO_2 concentration with overall variance explained greater than 98%.

Using this CO_2 loading and partial pressure data, a plot of $\ln(K_{eq})$ versus $1/T$ was generated (Figure 3). The values obtained for K_{eq} in this manner were found to exhibit the following Arrhenius dependence with temperature as:

$$\ln K_{eq} = 2.978 + \frac{2953.6}{T} \tag{3}$$

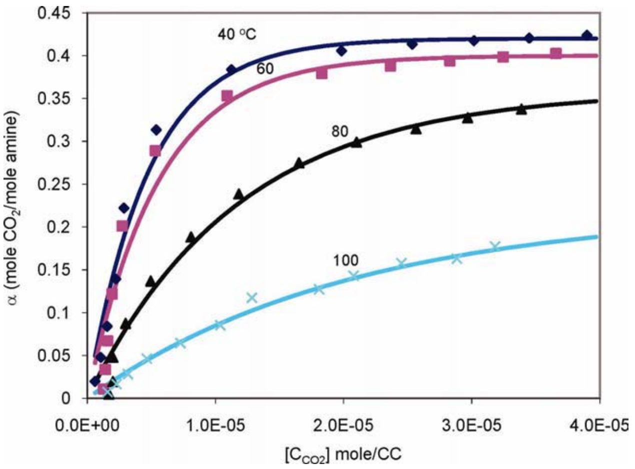

Figure 2. Curve fitting of Eq. 11 to experimental data to obtain K_{eq} and α_{max}.

[Color figure can be viewed in the online issue, which is available at wileyonlinelibrary.com.]

In general terms, the equilibrium distribution of CO$_2$ between an aqueous alkanol-amine solution and a vapor phase is determined by the solution of a set of equations comprising (1) two species balances, one for CO$_2$, and one the amine (C and N), (2) five reaction equilibrium equations for the dissociation of various species in solution, (3) an equation of electro-neutrality, and (4) isofugacity statements for each species which is present in both phases.[6] For example, the equilibrium chemical reaction for amine-CO$_2$ reaction is:

$$2R_1R_2NH + CO_2 \overset{K_{eq}}{\rightleftharpoons} R_1R_2NH_2^+ + R_1R_2NCOO^- \tag{4}$$

Mathematically, the corresponding equilibrium constant is defined in terms concentration:

$$K_{eq} = \frac{[R_1R_2NH_2^+][R_1R_2NCOO^-]}{[R_1R_2NH]^2[CO_2]} \tag{5}$$

Using this method, Weiland et al.[6] provided the following empirical expression for diethanolamine (DEA)-CO$_2$ reaction equilibrium constant as:

$$\ln K_{eq} = -8.502 + \frac{6801.7}{T} \tag{6}$$

The experimental data for equilibrium constant are illustrated alongside this empirical expression (Eq. 6) in Figure 3. The agreement in the values of the equilibrium constant was remarkable in that the empirical expression (Eq. 6) was developed from mathematical theory for DEA-CO$_2$ reaction in aqueous solution. Differences in the temperature dependence were expected due to the fact that the amines on the supported sorbent were a mixture of alkanol-amines. These results provided confidence in the validity of the technique presented here to obtained equilibrium constant.

The equilibrium CO$_2$ concentration, $C_{CO_2,eq}$, was obtained using following expression[7]:

$$[CO_2]_{eq} = \frac{1}{K_{eq}}\left(\frac{\alpha_{max}}{1-2\alpha_{max}}\right) \tag{7}$$

As a result of the reaction stoichiometry, the maximum CO$_2$ loading is 0.5 (Eq. 4). In the presence of moisture, this stoichiometry can change up to a value of unity. It is unclear how water in the matrix of a solid support or gas phase moisture in saturated flue gas will influence this stoichiometry. The maximum CO$_2$ upload, α_{max}, was obtained by combining the TGA α_{max} (Monazam et al., submitted) with those values measured experimentally from the volumetric sorption apparatus:

$$\alpha_{max} = 1.923 - 0.0048T \tag{8}$$

At the lower temperatures both α_{max} values approached the same asymptotic value. However, at higher temperatures (80–100°C), the TGA method values were somewhat lower than the volumetric α_{max}. This may be due to differences in the sample preparation. It was decided that the best approach was to simply combine the data sets. This explained 80% of the variation in the data.

The equilibrium CO$_2$ concentration, $C_{CO_2,eq}$, as a function of α_{max} using Eqs. 6 and 8 into Eq. 7 is illustrated by Figure 4. The vapor pressure of CO$_2$ over the sorbent saturated with CO$_2$ at α_{max} decreased as the loading, α_{max}, decreased. This is critical to determining the driving force for CO$_2$ capture into the amine supported sorbent.

The effect of reaction temperature on the fraction of CO$_2$ conversion for amine/bentonite particle of 70 μm diameter is illustrated in Figure 5. The CO$_2$ conversion, X, is defined as:

$$X = \frac{m(t) - m_o}{m_f - m_o} \tag{9}$$

where $m(t)$ is instantaneous weight of the solid during the exposure to CO$_2$, and m_o and m_f are initial and final weight, respectively. When the data is normalized in this way, it can clearly be seen that the rate of sorption increases with temperature. The only departure in this trend is the data taken at 40°C. The absorption of CO$_2$ at this temperature exhibits an absorption rate more characteristic of that observed at 60°C. It is hypothesized that there may be a complex interaction of the inherent water in the clay structure with the amines, which alters the stoichiometry and rate of CO$_2$ capture at this temperature. The standard error as calculated using the error bar option in

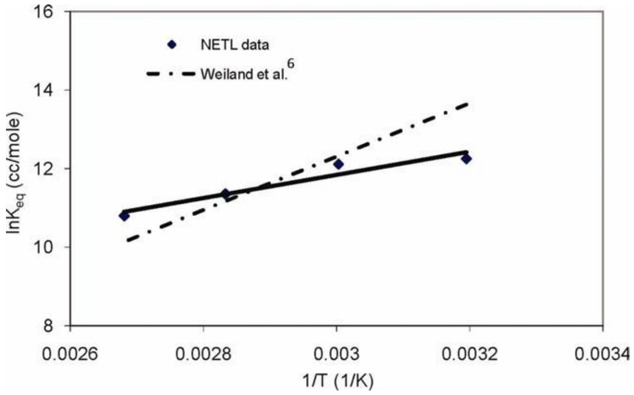

Figure 3. Comparison of K_{eq} between NETL data and Weiland et al.[6] correlation.

[Color figure can be viewed in the online issue, which is available at wileyonlinelibrary.com.]

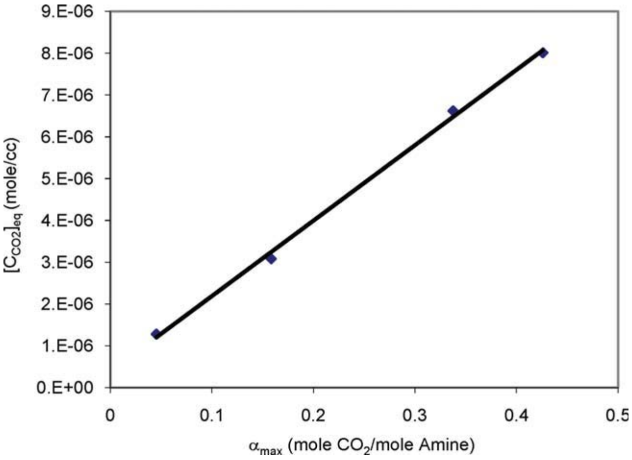

Figure 4. Variations of CO_2 concentration with CO_2 loading.

[Color figure can be viewed in the online issue, which is available at wileyonlinelibrary.com.]

Microsoft Excel 2007 has been added to the upper and lower temperature data points demonstrating that there is significant difference between various responses for different temperatures.

A heat of reaction was measured using a differential scanning calorimeter to be 77 J/g sorbent at 40°C. Using the equilibrium CO_2 uptake, the heat of reaction was about 64 kJ/mol of CO_2. The net absorption process was exothermic. This represents a rather significant quantity of heat release. The experiments conducted in the TGA were designed to thermally equilibrate rapidly so that the data can be analyzed as isothermal responses. Experiments were conducted on various particles size, sample sizes, and gas sweep rates. It was found that particles smaller than 100 μm, sample sizes less than 50 mg, and gas flows of greater than 50 ml/min produced repeatable and maximized the uptake of CO_2 over the testing period. As a result, the heats of reaction can be safely considered to be negligible and data analyzed as isothermal.

The major models that have been developed for noncatalytic fluid–solid reactions are the shrinking core, shrinking particle, grain boundary, and homogeneous models. The shrinking core model (SCM) is applicable to an initially nonporous particle, which reacts with a reagent leaving a reacted layer around the unreacted core. The shrinking particle model is similar to the SCM except that no product layer is left around the unreacted core. The grain boundary model is applicable to a solid consisting of individual dense grains compacted together, whereas the homogeneous model is applicable to a solid with a homogeneous distribution of pores. Among these models, the most common model used in the gas–solid reaction is SCM where the particle size would not change but the reacting core shrink inside the particle. In lieu of data on the particle size effects, the SCM appeared to be the most appropriate model for the amine supported sorbent.

The SCM was first developed by Yagi and Kunii.[8] In the establishment of the SCM, the solid reactant is considered to be nonporous and is initially surrounded by a fluid film through which mass transfer occurs between the solid particle and the bulk of the gas. As the reaction proceeds, an inert product layer forms around the unreacted core. Example of such systems are frequently encountered in chemical and metallurgical processes, such as the reduction of metal oxides, the oxidation of metals, the roasting of ores, and combustion and gasification of coal. Detailed derivation of the SCM can be found in Levenspiel[9] and Szekely et al.[10]

For the analysis of 70-μm amine supported sorbent, it was assumed that the solid particle is spherical and it reacts with the gas isothermally. Also, the concentration of the reacting gas was assumed to be constant or in excess.

The SCM is based on three different rate-controlling steps in the overall mechanism and, for spherical particles, the progress of reaction of a nonporous solid to product is shown schematically in Figure 6. As the reaction proceeds, the unreacted core diminishes. The reaction occurs at the surface representing the sharp interface between the unreacted core and the product layer.

As shown in Figure 6, the overall process consists of chemical reaction at the interface, and the diffusion of gaseous reactant and products through the solid–product layer and through the boundary layer at the external surface of the solid. The overall rate may be controlled by: (1) the rate of chemical reaction, (2) by the rate of diffusion, or (3) by both (1) and (2). In other words, the third controlling case is when the rate of chemical reaction is comparable with the rate of diffusion such that these two steps may produce comparable resistance to the progress of reaction, and so both contribute to the overall process of the reaction.

The relationships between time and fractional conversion are as follows:

The general reaction A(g) + bB(s) → Product is used in the development of the SCM:

(1) Gas film diffusion control:

$$\frac{t_{\mathrm{gas}}}{\tau_{\mathrm{gas}}} = X \tag{10}$$

where

$$\tau_{\mathrm{gas}} = \frac{R\rho_{\mathrm{b}}}{3bk_{\mathrm{g}}M_{\mathrm{b}}(C_{\mathrm{CO_2}} - C_{\mathrm{eq}})} \tag{11}$$

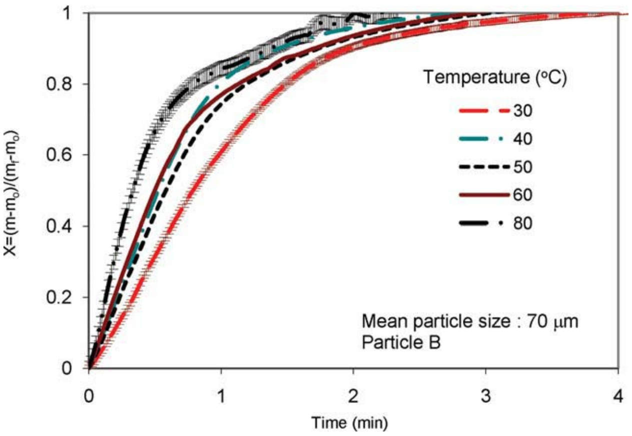

Figure 5. Effect of reaction temperature on CO_2 reaction with amine-based solid sorbent. Standard error is included on the 30 and 80°C test data points.

[Color figure can be viewed in the online issue, which is available at wileyonlinelibrary.com.]

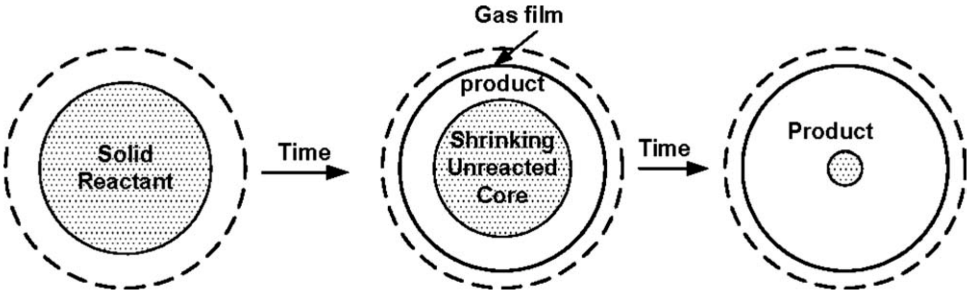

Figure 6. A gas–solid reaction proceeding with the formation of a shrinking unreacted core.

where k_g is the external mass-transfer coefficient. This external mass transfer through the gas boundary layer usually provides a negligible resistance to the progress of reaction and hence has only a small effect on the overall rate.[10]

(2) Diffusion through the product solid layer control:

$$\frac{t_{\text{diff}}}{\tau_{\text{diff}}} = 1 + 2(1-X) - 3(1-X)^{2/3} \tag{12}$$

Equation 12 may also be written in explicit form as[11]

$$X = 1 - \left[\frac{1}{2} + \cos\left[\frac{\pi}{3} + \frac{1}{3}\cos^{-1}\left(1 - \frac{2t_{\text{diff}}}{\tau_{\text{diff}}}\right)\right]\right]^3 \tag{13}$$

where

$$\tau_{\text{diff}} = \frac{R^2\rho_b}{6bD_eM_b(C_{CO_2} - C_{eq})} \tag{14}$$

where D_e is the diffusion coefficient for CO_2 through the product layer.

(3) Chemical reaction control at the surface of the unreacted core

$$\frac{t_{\text{Rxn}}}{\tau_{\text{Rxn}}} = 1 - (1-X)^{1/3} \tag{15}$$

Equation 15 may also be written in explicit form as:

$$X = 1 - \left(1 - \frac{t_{\text{Rxn}}}{\tau_{\text{Rxn}}}\right)^3 \tag{16}$$

where

$$\tau_{\text{Rxn}} = \frac{R\rho_b}{bk_sM_b(C_{CO_2} - C_{eq})} \tag{17}$$

And k_s is the surface reaction rate constant. Note that each of the characteristic times is dependent on the particle size; the reacted layer diffusion time is dependent on R^2.

In general, more than one resistance influences the conversion of the particle. Thus, combining the three individual rate expressions gives the instantaneous rate of reaction, whereas the particle is being converted:

$$\dot{R}''(\text{mol/cm}^2\ \text{s}) = \frac{b(C_{CO_2} - C_{eq})}{\frac{1}{k_g} + \frac{R}{D_e}\left(\frac{1}{\xi} - 1\right) + \frac{1}{k_s\xi^2}} \tag{18}$$

where $\xi = r_c/R = (1 - X)^{1/3}$.

The time needed to reach any particular conversion is given as:

$$t_X = \tau_{\text{gas}}X + \tau_{\text{diff}}\left[1 - 3(1-X)^{2/3} + 2(1-X)\right] + \tau_{\text{Rxn}}\left[1 - (1-X)^{1/3}\right] \tag{19}$$

The kinetic regime of the reaction can also be identified[10] by the modulus, σ^2:

$$\sigma^2 = \frac{\tau_{\text{diff}}}{\tau_{\text{Rxn}}} \tag{20}$$

This is defined as the ratio of the internal diffusion and intrinsic reaction resistances. The reaction is diffusion control if $\sigma^2 > 10$ and intrinsic chemical reaction-control if $\sigma^2 < 0.1$.

To quantify the effect of temperature on reactivity of amine/bentonite in CO_2 capture, the experimental conversion time for each reaction temperature was compared with the ideal chemical reaction and product diffusion control models. The conversion-time fitted more closely to the chemical reaction control for the temperatures up to 40°C (Figure 7). These comparisons suggested that chemical reaction kinetics controlled the rate of reaction at low temperatures. Figure 7 also shows that for higher reaction temperature (>90°C), the conversion-time data fitted more closely to the product diffusion control and, therefore, indicated that the reaction was controlled by product layer diffusion. The reaction at temperature between 60°C and 90°C

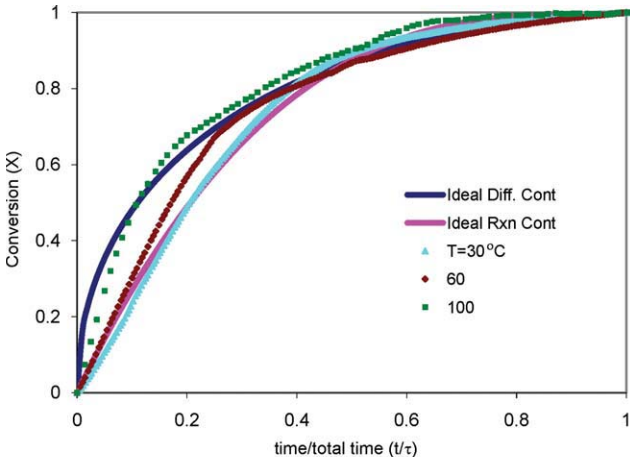

Figure 7. Comparison of reaction rate to different reaction models at T = 30, 60, and 100°C.

[Color figure can be viewed in the online issue, which is available at wileyonlinelibrary.com.]

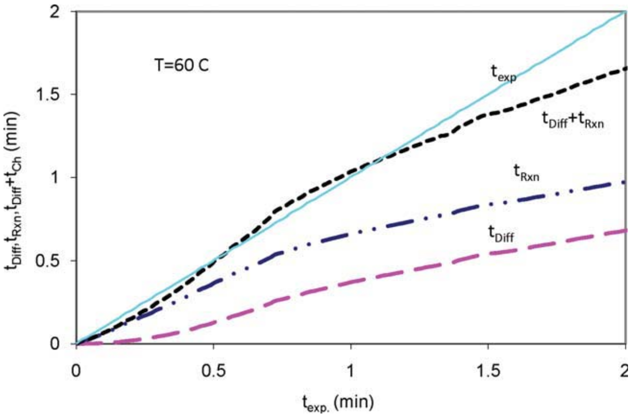

Figure 8. Analysis of diffusion and reaction time in respect to experimental time at T = 60°C.

[Color figure can be viewed in the online issue, which is available at wileyonlinelibrary.com.]

was neither completely chemical reaction nor diffusion controlled processes; both steps contribute significantly to describing the overall process rate. The temperature responses agree with the theoretical responses for the diffusion and chemical reaction control within the standard errors reported in Figure 5 for the upper and lower temperature data.

In this work, it was assumed that external mass transport was fast and the overall rate of reaction could be expressed in terms of the rate of chemical reaction and the rate of diffusion through the product layer. Using experimental conversion-time data and fitted to Eq. 19, the two unknowns (τ_{diff} and τ_{Rxn}) were obtained using least-squares method of minimization. The modeled diffusion and reaction times are shown in Figure 8 for reaction temperature of 60°C relative to the experimental time. To reproduce the experimental time the diffusion and reaction time must be summed together, demonstrating that at 60°C both contribute significantly to the overall reaction rate.

The values of D_e and k_s were obtained for amine/bentonite particle B of 70 μm in diameter taking the modeled diffusion and chemical reaction times for each temperature. The temperature dependence for these extracted values D_e and k_s were fitted to the Arrhenius equations ($R^2 > 94\%$), as shown in Figure 9. The fit for D_e and k_s produced the following effective diffusivity and surface reaction kinetics:

$$D_e(\text{cm}^2/\text{s}) = 6.823 \times 10^{-5} e^{\frac{-1.6275}{RT}} \tag{21}$$

and

$$k_s(\text{cm/s}) = 28.2 e^{\frac{-6.35}{RT}} \tag{22}$$

The frequency factor of 28.2 and activation energy of 6.35 kcal/mol were consistent with amine based weak ionic reaction with CO_2 as observed when kinetics are measured in solution.

Conclusions

In this study, a rigorous approach has been taken to describe the equilibrium and surface CO_2 absorption rate using solid supported amine sorbents. A SCM was used to interpret absorption data taken between 30 and 120°C in TGA and equilibrium volumetric sorption apparatus. The maximum CO_2 loading on the clay supported sorbent was determined using both the gravimetric and volumetric techniques. The experiments were designed to minimize complicating thermal and mass transfer effects. An expression was developed using both test data describing the relationship between maximum capacities as a linear function of temperature. The vapor pressure of CO_2 in equilibrium over the sorbent was measured and the temperature-dependent equilibrium constant was reported. An Arrhenius model for the prediction of CO_2 equilibrium was successfully used to fit a series of experimental data on CO_2 loading at various temperatures (303–363 K) and CO_2 partial pressures (10–760 mm Hg) obtained from volumetric adsorption apparatus.

The capacity of the sorbent to hold CO_2 decreased with reaction temperature as indicated by the maximum value presented in Figure 2. Thus, the extent of reaction as it approached equilibrium varied inversely with temperature. This was also confirmed from TGA data and both results when combined lead to the formulation of Eq. 8. This reaction was measured to be exothermic with an enthalpy of reaction 64 kJ/mol of CO_2. According to LeChatelier's principle, an increase in temperature shifts the extent of reaction in favor of the reactants for such an exothermic reaction (Eq. 4). However, this should not be misconstrued as an indication that the rate decreases with temperature. The test data reported in Figure 5 indicated an increasing rate with increasing temperature. This was used to extract the temperature-dependent kinetic parameters for both chemical kinetics, k_s, and diffusion coefficient, D_e (Figure 9). Thus, both chemical kinetic and diffusion resistances were, in fact, found to be lower at higher temperatures.

The diffusion coefficient and surface chemical kinetic parameters were extracted from the TGA test data taken over the same range of temperatures. Comparative analysis of CO_2 absorption over the entire temperature range demonstrated that these competing processes both contribute to the absorption behavior. By calculating the dependence of the diffusion and chemical reaction times on the temperatures, the extent of conversion of the reaction data could be compared with the reaction model varying the fitted parameters. Using a least-squares method of minimization iteration method, parameters for the diffusion coefficient, frequency factor, and the activation energy were estimated. The values obtained indicated that for these 70 μm amine supported sorbents diffusion processes dominated at high temperatures characteristic of

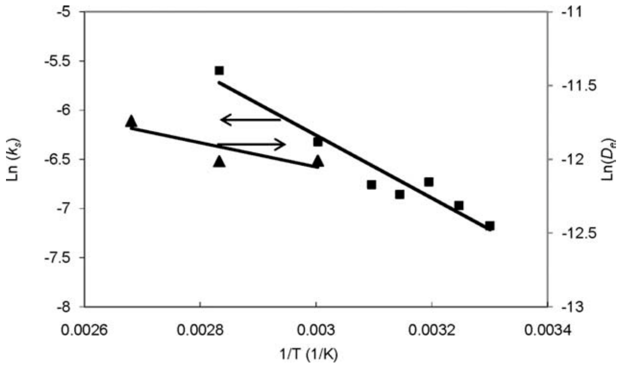

Figure 9. Temperature dependence of the chemical reaction rate, k_s (cm/s), and effective diffusion-rate coefficient, D_e (cm^2/s).

regeneration processes (80–100°C), whereas chemical kinetics controlled at the lowest temperatures (30–40°C). At the intermediate temperatures, the process rate was found to be a mixed contribution of both diffusion and chemical reaction rates.

It is in this intermediate range where commercial processes are projected to be needed to retrofit existing power plants, it was found that both diffusion and chemical processes contribute to controlling the process rate. Thus, when considering particle sizes which are suitable for this scale process equipment, it is important to incorporate both mass transport and chemical rate processes. For larger particle sizes and larger bed volumes required in commercial applications, the temperature range and contribution of the mass and thermal transfer processes will vary. More work is required on mass-transfer rates for larger particles to confirm the applicability of these diffusion and kinetic models to those process conditions.

Acknowledgments

The authors thank the Department of Energy for funding the research through the Fossil Energy's Carbon Sequestration/CO_2 Capture Research program.

Notation

A = reacting gas
b = mole of B consumed per mole of A reacted (dimensionless)
B = component of solid reacting with gas
C_{CO_2} = CO_2 concentration of gaseous product (mol/cm^3)
C_{eq} = equilibrium concentration (mol/cm^3)
D_e = diffusion coefficient of the gaseous phase (cm^2/s)
k_s = surface reaction rate constant (cm/s)
K_{eq} = equilibrium constant (cm^3/mole)
k_g = mass-transfer coefficient (cm/s)
M_b = molecular weight of reacting solid
R = particle radius (cm)
R_1 = primary amine, $CH_2CH_2OH{=}C_2H_4OH$
R_2 = secondary amine, $R_2 = R_1$ for DEA and $R_2 = H$ for MEA
t = time of reaction (min)
t_{gas} = gas film diffusion time (min)
t_{Diff} = diffusion through the product layer time (min)
t_{Rxn} = chemical reaction control time (min)
T = temperature (K)
X = conversion

Greek letters

α_{CO_2} = CO_2 loading (mole CO_2/mole amine)
ρ_b = density of solid reacting with gas (g/cm^3)

Literature Cited

1. Rao AB, Rubin ES. A technical, economic, and environmental assessment of amine-based CO_2 capture technology for power plant greenhouse gas control. *Environ Sci Technol.* 2002;36:4467–4475.
2. Hoff AK, Mejdell T, Juliussen O, Børresen E, Lauritsen GK, Semb TH, Svendsen FH. Solvents selection for a post combustion CO_2 capture process. In *Proceedings of the GHGT-8: 8th International Conference on Greenhouse Gas Control Technologies*, Norway: Trondheim, June, 2006:6; paper 01_06_08, PDF.
3. Siriwardane RV, Robinson C. Liquid-impregnated clay solid sorbents for CO_2 removal from post combustion gas streams. *J Environ Eng*. 2009;6:378–385.
4. Yang W-C, Hoffman J. Exploratory design study on reactor configurations for carbon dioxide capture from conventional power plants employing regenerable solid sorbents. *Ind Eng Chem Res*. 2009;48:341–351.
5. Siriwardane RV, Shen MS, Fisher EP, Poston JA. Adsorption of CO_2 on molecular sieves and activated carbon. *Energy Fuels*. 2001;15:279–284.
6. Weiland RH, Chakravarty T, Mather AE. Solubility of carbon dioxide and hydrogen sulfide in aqeous alkanolamines. *Ind Eng Chem Res*. 1993;32:1419–1430.
7. Alatiqi I, Sabri MF, Bouhamra W, Alper E. Steady-state rate-based modeling for CO_2/amine absorption-desorption systems. *Gas Sep Purif*. 1994;8:3–11.
8. Yagi S, Kunii D. *Studies on combustion of carbon particles in flames and fluidized beds*. In: *Fifth Symposium (International) on Combustion*. New York: Reinhold, 1955:231–244.
9. Levenspiel O. *Chemical Reaction Engineering*, 3rd ed. New York: Wiley, 1999.
10. Szekely J, Evans JW, Sohn HY. *Gas Solid Reactions*. New York: Academic Press, 1976.
11. Ruthven DM. *Principles of Adsorption and Adsorption Processes*. New York: Wiley-Interscience Publication, 1984.

Manuscript received Jun. 7, 2010, revision received Oct. 20, 2010, and final revision received Dec. 7, 2010.